Gaze-Shifting in Humans and Humanoids

Eric Mousset[1], Marwan Jabri[1], Simon Carlile[2], and Terrence Sejnowski[3]

[1] Computer Engineering Laboratory, School of Electrical and Information Engineering, The University of Sydney, NSW 2006 Australia
[2] Auditory Neuroscience Laboratory, Department of Physiology, The University of Sydney, NSW 2006 Australia
[3] Computational Neurobiology Laboratory, The Salk Institute for Biological Studies, 10010 North Torrey Pines Road, La Jolla, CA 92037, USA

Abstract. The seemingly simple act of moving the line of sight in a new direction in order to attend to a salient event in one's direct surrounding involves multiple computational tasks, such as (visual) novelty detection, target selection, integration of spatial information originating from multiple sensory modalities (visual, auditory and/or somatosensory) and precise coordination of head and eye motor control. The present study consists of a computational modeling approach of some sensorimotor principles of gaze-holding and gaze-shifting in humans. A review of related biological observations is provided, that emphasizes how crucial the understanding of the functioning of the neural circuitry for gaze-shifting is for the design of humanoid robots. Particular attention is given to how close the model's sensorimotor responses (such as eye movement dynamics and saccadic reaction time) are from their biological counterparts. Experimental illustrations of these behaviors include tests of a stand-alone version of the model using simple synthetic signals as well as real-world scenarios confronted to its implementation on a Nomadic Technologies XR4000 robotic platform. Experimental results serve as a basis of a discussion presenting our work as a building block for further investigations and developments of gaze-shifting functionalities, or more generally, sensorimotor capabilities, in humanoid robots.

1 Introduction

The design of humanoid robots raises significant issues, such as how to handle the intrinsic complexity of real-world signals with limited sensory and computational resources, and how to react to them with efficient sensorimotor strategies. Unlike conventional robotics, the concern here does not restrict to the range of tasks that a given robot is able to achieve but also extends to how those tasks are achieved, that has to resemble as much as possible the human way.

In this regard, the understanding of the neural system and the biomechanics of gaze-holding and gaze-shifting in humans is particularly important, and this for many reasons. First of all, this system acts as a dynamic, non-homogeneous sampling gate between the exterior visual scene and the higher-level cognitive functions of the central nervous system; the control exerted by the latter being only partial (in other words, the largest majority of eye-movements are not voluntary). It embeds lower-level computational mechanisms for

- target selection (amongst several simultaneous, behaviorally-significant visual events, what particular target should be attended next?),
- movement-programming (how should the parameters of the next movement be calculated?),
- gaze-holding (how long should the fovea remain fixating?),
- sensory fusion (how should the spatial information coming from visual, auditory and somatosensory modalities be combined), and
- coordinated motor control of eye and head trajectories.

The present paper focuses on the subpart of the gaze-shifting system relative to visually-triggered, high-velocity (up to 900 degrees per second in Man), "reflexive", eye-movements (commonly referred to as optic saccades or saccadic eye-movements). Unlike many other functional sub-systems of the human brain, the neural areas that control eye movements form a closed, well-defined system. Moreover, there is a fairly high degree of similarity of structural organization across mammalian species (and even higher between humans and primates). Extensive, quantitative experimental data on the neural pathways for optic saccades in primates have been collected over the last three decades (for a review, see [21, 66]) that are directly beneficial to the understanding of these principles in humans. This stream of fundamental biological investigations has given rise to a substantial amount of computational modeling approaches concerning mammals [11, 12, 18, 30, 38, 43, 47, 52, 61] and avians [27, 58].

The main motivation of this study is twofold. On the one hand, it aims at linking neural structure with behavioral function. On the other hand, it identifies which neural computational strategies are of particular interest for the

design of human-like systems. The rest of the paper organizes as follows. Section 2 consists a brief overview of related biological studies followed by the presentation of our own modeling work on the collicular pathway for optic saccades in monkeys (including retinal ganglion cells, superficial and deeper layers of the Superior Colliculus, and brainstem). Section 3 describes the implementation of this model on a Nomade XR4000 robotic platform (Nomadic Technologies). The description of the experimental setup the presentation of the corresponding results are found in sec.4. More general issues regarding the implementation of gaze shifting principle in humanoids are discussed in sec.5.

2 Computational Modeling of the Saccadic System in Primates

2.1 Structure and Function of the Saccadic System

Superior Colliculus. Over the last three decades considerable experimental research has been carried out concerning the detailed functioning of the primate oculomotor saccadic system. This has resulted in thorough anatomic and functional descriptions of the neural pathways between the retina and the oculomotor muscles. The pathway including the superior colliculus (SC), the brainstem and the cerebellum (Fig.1A) plays a significant, if not the most significant, role in the production of saccadic eye-movements. At the sensory level, unlike the visual cortex,
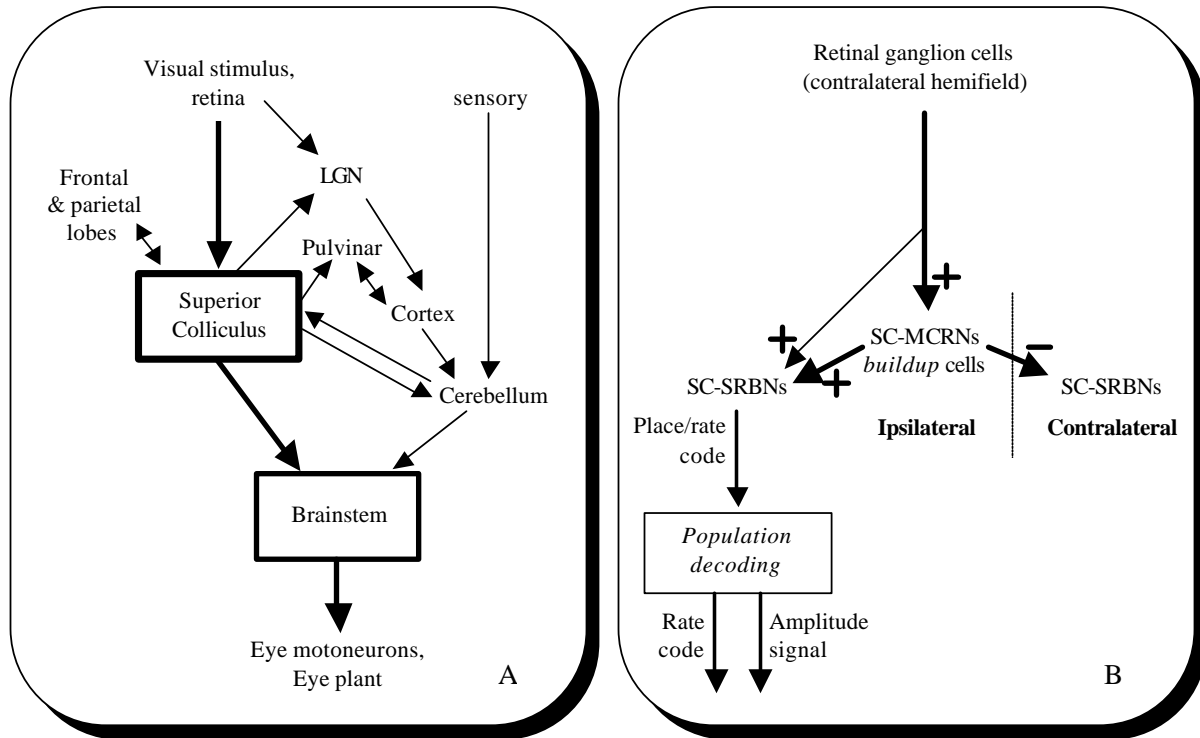
Fig. 1. Box A: Main pathways and brain areas for the programming and control of gaze shifting. Thick arrows and boxes delineate the main focus of the present modeling study. **Box B: Target selection and saccade programming in the collicular pathway.** Contralateral inhibitions between both colliculi ensure a lateral, mutually exclusive programming of the saccade. Saccade metrics and dynamics are determined downstream of SC, by the *population decoding* unit. SRBNs: Saccade-Related Burst Neurones. MCRNs: Movement-Coding Related Neurones (alternatively refered to as either *buildup* or *fixation* cells in [45] according to their location on the rostro-caudal axis).

the SC receives a direct projection from retinal ganglion cells. In terms of number of synaptic contacts, the collicular pathway is the shortest pathway between retinal neurons and oculomotor neurons. As a result, it is responsible of shortest reaction times, ranging from 70ms to 90ms in monkey [16, 59], and from 90ms to 120ms in human [17, 22] under normal conditions. Either saccade latency or saccade duration (or both at once) dramatically deteriorate if the SC is lesioned [16, 65] or pharmacologically deactivated [1]. Aside from purely visual responses, SC also includes monosensory and multisensory cells coding for visual, auditory and/or somatosensory modalities

[40]. Topographic maps for each of these three modalities coexist and are aligned with one another. The SC is actually the only area where a two-dimensional (azimuth, elevation) map of the auditory space has been observed [35]. At the motor level, cell populations of the deeper layer of the SC encode a gaze-shift motor map. Their direct electrical microstimulation during fixation induces a saccadic eye-movement in the head- restrained animal or an eye-head coordinated gaze-shift if the head is unrestrained; the amplitude and direction of the stimulation-evoked movement depending on both the site and parameters of the excitation [51, 55, 60, 67]. Moreover, recent studies on the human visual attention have revealed the contribution of midbrain structures (such as SC and pulvinar) on cognitive visual processing, probably due to the projections sent by SC to the secondary cortical visual areas through the pulvinar [9, 53].

In summary, the SC plays a pivotal role in the generation of saccades. On the one hand, the collicular pathway for saccade generation is partially modulated by the frontal lobe structures (through SC) and on the other hand the SC partially influences higher-level, visual, cognitive analysis. All these observations, taken together, show how crucial the understanding of the functioning of the collicular pathway is for the comprehension of gaze-shifting principles in man and their application to the design of humanoid robots.

Brainstem. The functional organization of the brainstem, the brain area responsible for the motor control of saccadic eye-movements, has been the most widely studied of all oculomotor subsystems [26, 32]. The neural code that it produces (remarkably similar to the velocity profile of the eye-movement itself) is transformed at the level of the oculomotor nucleus into an appropriate excitation pattern that drives the oculomotor muscles and enable them to perform high-velocity movements with dramatic accuracy. However, saccade velocity is so high (up to 900 degrees per second in Man), and duration so short (as little as 25msec in Man), that any feedback signal originating from the retina would reach the brainstem with a delay too long to possibly influence the ongoing control of the movement. Nor does accuracy depend on proprioceptive feedback from extraocular muscles [23, 34]. In what is considered a milestone in the modeling of the saccadic system, Robinson proposed the so-called local feedback controller model [57], where an estimate of the motor error is formed at the level of the brainstem and compared to the desired command. Since then, this concept has been subject to numerous refinements [5, 18, 30, 42, 61]. A major variant has emerged, that considers SC as part of the feedback loop [3, 13, 37, 50, 71, 72].

Cerebellum. Over the last two decades, experimental evidence has accumulated demonstrating the importance of the role of the cerebellum in the control of saccadic eye-movements; especially works concerning the effects of cerebellar lesions. Since then several modelling investigations have aimed at accounting for mechanisms of compensation for alterations of the oculomotor plant due to fatigue, age or injury [12, 20, 49]. Additionally, the cerebellum has recently been proposed to act as a key-component of the local feedback loop for the control of saccadic eye- movements by performing the temporal integration of the spatial displacement [52]. Consistent with these previous studies the model described here identifies the superior colliculus, the brainstem and the cerebellum as the principal components involved in the preparation and control of saccadic eye-movements (Fig.1A).

Target Selection. Saccade parameters such as latency and amplitude are modulated according to the configuration of the visual scene (e.g. onset, offset, shape and relative position of visual events). Recent quantitative studies have revealed that when presented within about 20 degrees of the target axis (and in the same visual hemifield), distractors significantly affect saccade amplitude (the eye reaches an average location between the target and the distractor) but not latency [74]. Reciprocally, when distractors are presented outside this 40deg window, saccade amplitude is not affected whereas significant latency increase is observed. The results of a recent, thorough study add support to the hypothesis where these processes occur downstream of the deeper layer of the Superior Colliculus, at least as far as express saccades are concerned [14].

2.2 Model Architecture and Function

Ganglion Cells & Retinal Spatio-Temporal Sampling. In the present study, the main focus is on the information processing happening downstream of the retina. Henceforth, the modeling of the retinal processing itself has been simplified in order to only account for properties which are important to the concerned downstream analysis:

1. The spatial sampling operated at the level of the ganglion cells is not uniform and varies exponentially according to eccentricity (with maximum resolution and minimum size of the receptive fields at the center of the fovea; see (3) in sec.7.2),

2. The temporal dynamics of ganglion cell is such that their activity exponentially decays over time when the photoreceptor stimulation pattern remains static (see (4) in sec.7.2);
3. 'Gray-level' information only is considered.

The retinal ganglion layer is the input structure for the whole model, as shown in Fig.1B. Detail on the its connection scheme between the upstream photoreceptor layer and downstream deeper layer of the Superior Colliculus are given Fig.2.

Saccade Preparation. The deeper layer of the SC has been known for a long time to embed a retinotopic motor map [55]. Eccentricity is (logarithmically) encoded along a rostro-caudal axis, and orientation along a media-lateral axis (the foveal region being represented at the rostral pole). The thorough electrophysiological study of this two-dimensional topographic layer has revealed the existence of several functionally distinct types of cells [45]. Various classifications (and corresponding labels) have been proposed according to the properties of their respective spatio- temporal discharge patterns and how these properties relate to saccade dynamics and metrics [2, 46]. Some cells are characterised by closed movement fields (i.e. a selectivity for movements of amplitude and direction in a restricted range) and by a solid burst of activity whose onset and offset is tightly correlated to saccade onset and offset, and henceforth are commonly referred to as Saccade-Related Burst Neuron (SRBN). In a typical saccade-related scenario, the burst of activity of SRBNs is preceded by a long prelude of activity in other cells of the SC deeper layer (up to several hundreds of milliseconds), henceforth labeled as Buildup Neurons in [45]. Buildup neurons are characterised by open movement fields, as the range of saccade amplitudes they respond to has typically no upper bound [2, 46]. Often refered to as fixation cells, the neurons located at the most rostral positions of this layer seem to fire in two different situations (some cells firing in both cases, alternatively): very small eye-movements and saccade prevention [15, 36, 45, 73]. Because of the movement-encoding role we are presenting in this paper, we propose to relabel these two latter groups of cells caudal (resp. rostral) Movement-Coding Related Neurons (cMCRNs resp. rMCRNs). Recent studies of SC intrinsic circuitry support the existence of a local network of inhibitory interneurons that may help shape the reciprocal discharge pattern between rMCRNs (fixation cells) and cMCRNs (buildup cells) and SRBNs [44, 41]. These are represented in the model as the three inhibitory connections from and to rostral MCRNs (see Fig.3).

An example of a typical scenario of achievement of a simple horizontal saccade is given in Fig.4. In absence of visual event, or for a stimulus located at the center of the fovea, the only active group of cells at the level of SC deeper layer are rostrally located MCRNs. The onset of a point-source visual stimulus results in two concurrent effects (see Fig.1B). (1) The direct projection from retinal GCs to SC-SRBNs induces the corresponding, retinotopic, spatial encoding and brings the potential of the latter to a level closer to (yet lower than) threshold. (2) A buildup of activity begins in the MCRN lamina, which also contributes to SC-SRBN facilitation. Eventually, the buildup of activity in the MCRN lamina reaches a level that triggers the burst of activity in SRBNs. This sudden raise of activity (that will remain high until full completion of the saccade) has three main consequences. (1) It causes rostral SC-MCRNs to stop firing. (2) The latter cessation of activity, combined with SRBN bursting, also causes brainstem OPNs to become silent and consequently 'open the gate' to a new motor command signal. (3) SC-SRBN burst of activity provides the necessary drive to LLBNs (and indirectly to EBNs) to produce the appropriate motor command. The rest of the brainstem saccadic circuitry (as depicted Fig.3) achieves the movement according to the desired displacement encoded at the level of SC-SRBNs (place code). When the saccade is completed, an external signal is sent to rostrally located MCRNs. The latter restart firing and consequently stop the bursting activity of SRBNs, and gradually inhibit caudal MCRNs. Rostrally located MCRNs will remain active until the next saccade.

Production of Saccades in the Azimuthal Plane. In the present model, the site for the calculation of the *desired displacement* and *rate code* signals used by the brainstem saccadic circuitry is located downstream of SC (see the *population decoding* functional unit Fig.3) as proposed in [14] and suggested in [64]. These calculations are performed in a neural network that, like SCd, is retinotopically organized (see equations and implementation details in sec.7.3.

Consistently with recent anatomic data our model features an excitatory projection from rostral SC-MCRNs onto the brainstem Omnipause Neurons (OPNs) ([8, 19, 29]. The model also includes a projection from caudal SC-MCRNs to OPNs, as suggested in [15, 29]. The third type of projection from SC deeper layer onto OPNs originates from SRBNs via inhibitory interneurons [15, 54] (see Fig.3).

The major projection of the SC SRBNs to the brainstem is commonly agreed to occur at the level of the saccade-related Long-Lead burst Neurons (LLBNs) [24, 25, 39, 63]. LLBNs serve as interneurons between collicular efferents and Excitatory Burst Neurones (EBNs). Their principal physiological feature consists of a prelude of activity

$\frac{d}{dt}\big(ph_{k,l}(t_n)\big)$

s_s

$W_{k,l}^{q,r}$

s_c

$d_{k,l,r,q}$

k

r

q

C_y

Photoreceptor array

C_x

l

$r = K \cdot \left(\exp\left(\frac{r-0.5}{B}\right) - 1 \right)$

$q_{\text{deg}} = 90 - \frac{180 \cdot (q-0.5)}{Q}$

orientation
(spans 360 deg)

Left hemifield

$q : 1 \leq q \leq Q$

90 deg

eccentricity

Right hemifield

Retinal ganglion cell array

To right-hemisphere SC

$r : 1 \leq r \leq R$

orientation, SCd rostro-caudal axis
(spans 180 deg)

Left hemisphere SC

$q : 1 \leq q \leq Q$

0 deg

eccentricity
SCd rostro-caudal axis

$r : 1 \leq r \leq R$
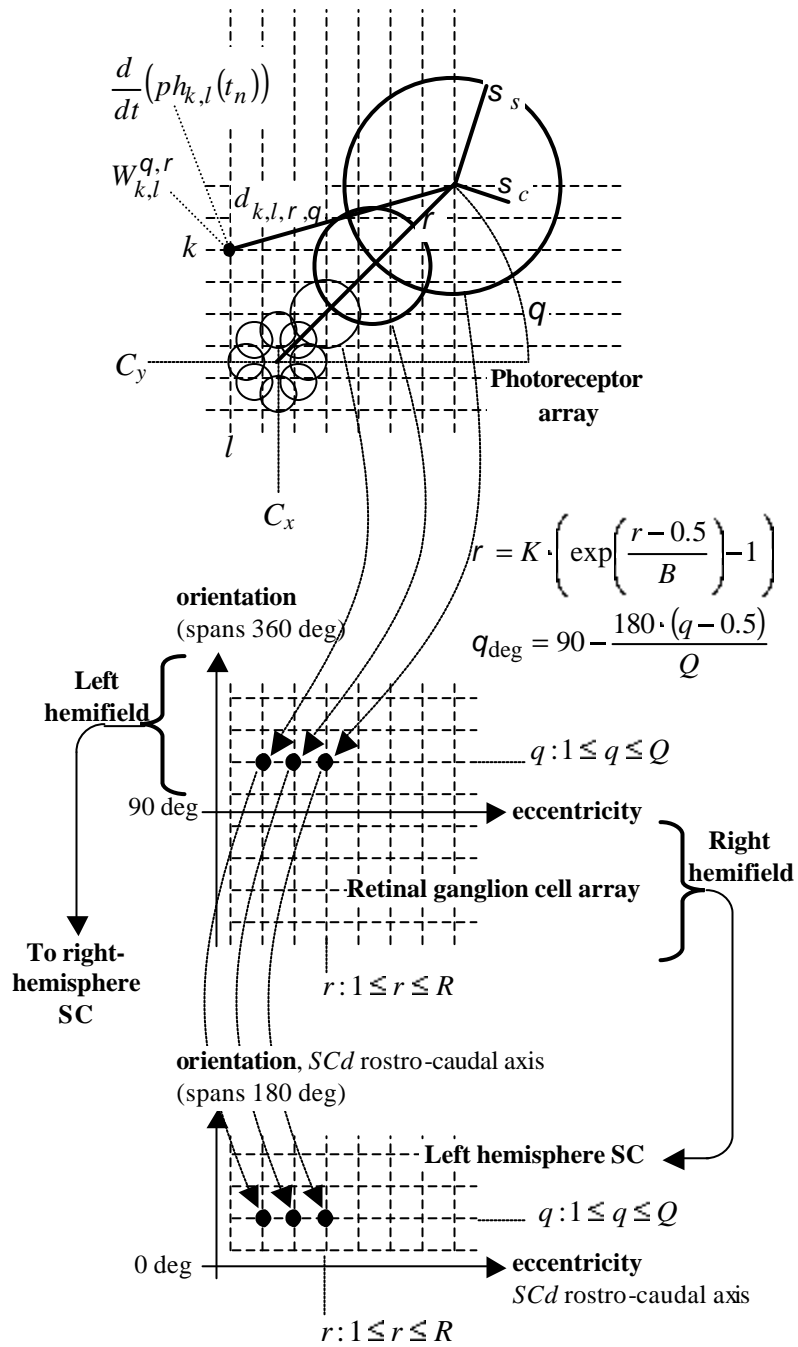
Fig. 2. Photoreceptors (PRs), retinal Ganglion Cells (GCs) and the SC deeper layer (SCd). The activity of the GC array (middle) is computed as the convolution between the PR array (top) and GC receptive fields. The spatial sampling operated by these receptive fields varies exponentially according to eccentricity (with highest density and lowest size at the center of the visual field). For sake of simplicity registered, one-to-one connections between GCs and SCd are hypothesized, yielding the well-known retinotopic organization of SCd (where the foveal regions projects to the rostral pole). See relating equations and implementation details in sec.7.2.
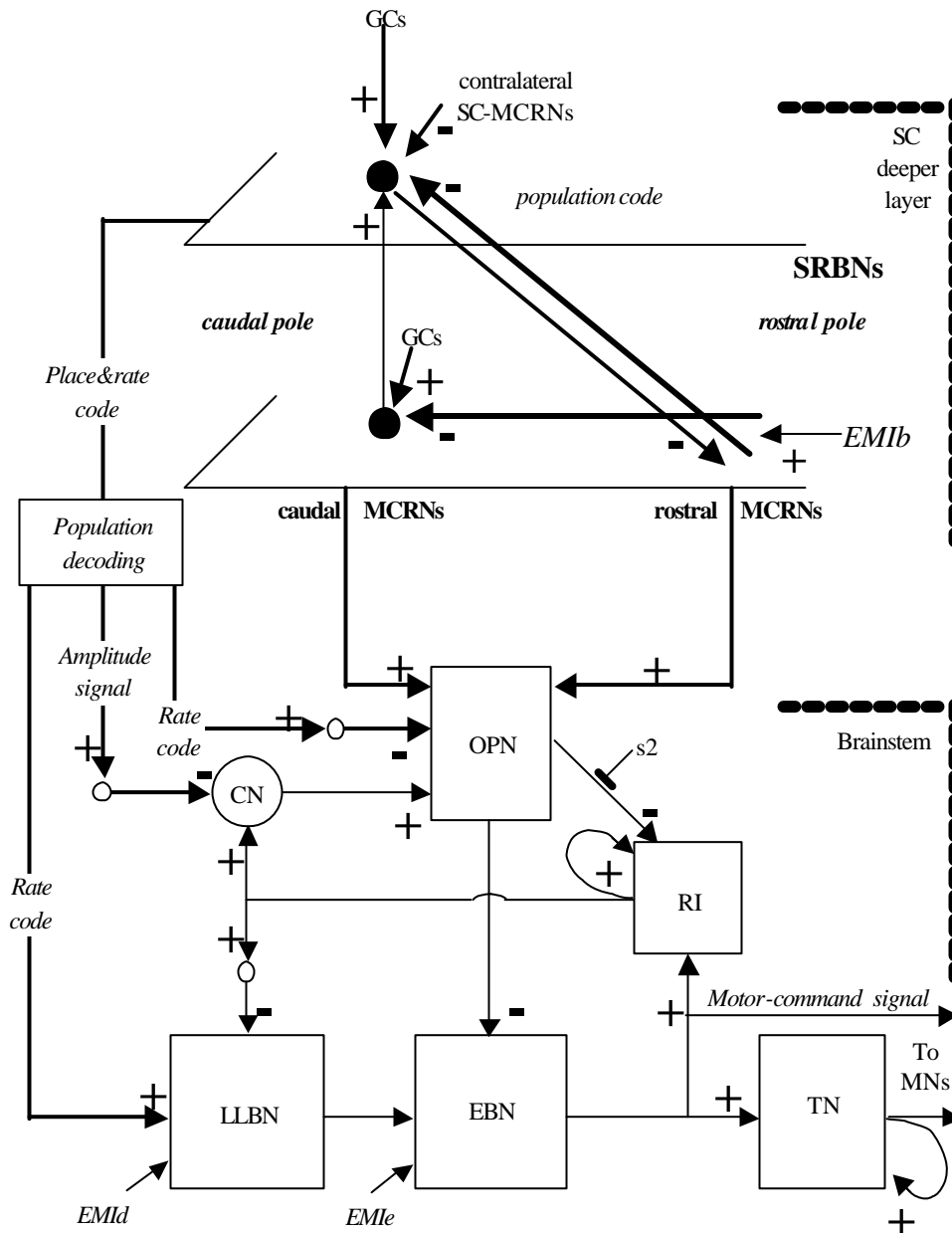
Fig. 3. Structure and connectivity between and within saccade-related neuron populations of both Superior Colliculus and Brainstem. The Superior Colliculus (SC) intermediate layer contains saccade-related laminae which are topographically organized and aligned. The Saccade-Related Burst Neurons (SRBNs) have closed movement fields and high-frequency discharges clipped to the saccade temporal boundaries. Rostrally located Movement-Coding Related Neurons (MCRNs) are active during fixation periods whereas caudally located cells have a reciprocal temporal profile. SC-SRBNs project to the brainstem and modulate its activity by delivering rate and place codes. Long-Lead burst Neurons (LLBNs) drive Excitatory Burst Neurons (EBNs), whose output forms the direct motor command of Tonic Neurons (TNs) and ocular Motoneurons (MNs). TNs integrate EBN motor command. A local, dynamic motor-error control loop takes place at the level brainstem by means of a Resetable Integrator. The latter integrates EBN discharge, gradually inhibits LLBNs as the movement proceeds and also delivers their signal to Comparator Neurons (CNs), which in turn contribute to reactivating OPNs once the motor-error is close to zero (by comparing the displacement integrated by RI to the desired displacement encoded in SC-SRBNs). OPNs projects to and inhibits both EBNs and RI. While the former inhibition is sufficiently strong to silence EBNs (and hence stop the saccade) in a very short amount of time, the latter is only gradual. External Modulating Inputs (EMIb, EMId and EMIe) are significant modulating signals from nuclei exterior to both SC and brainstem.

whose duration can range from a few milliseconds to several hundreds according to the behavioural context. Such a projection is part of the model (see leftmost arrow in Fig.3). Both LLBNs and EBNs are known to receive inputs from cell populations other than SC-SRBNs and LLBNs respectively (for a review, see [32]), which are summarized in the model as the External Modulating Inputs EMId and EMIe. An example of the effect of such a modulation is shown Fig.5. In addition, EBNS are known to project to the ipsilateral abducens nucleus which contains ocular motoneurons [7, 69, 70]. This projection is also modeled; see the EBN to MN arrow at the bottom right of Fig.3. Once the eye has reached its programmed destination, the oculomotor neurons need to be provided with a tonic signal in order to maintain the eye in a particular position. Therefore a velocity- to-position integration occurs at the level of the Tonic Neurons (TNs).
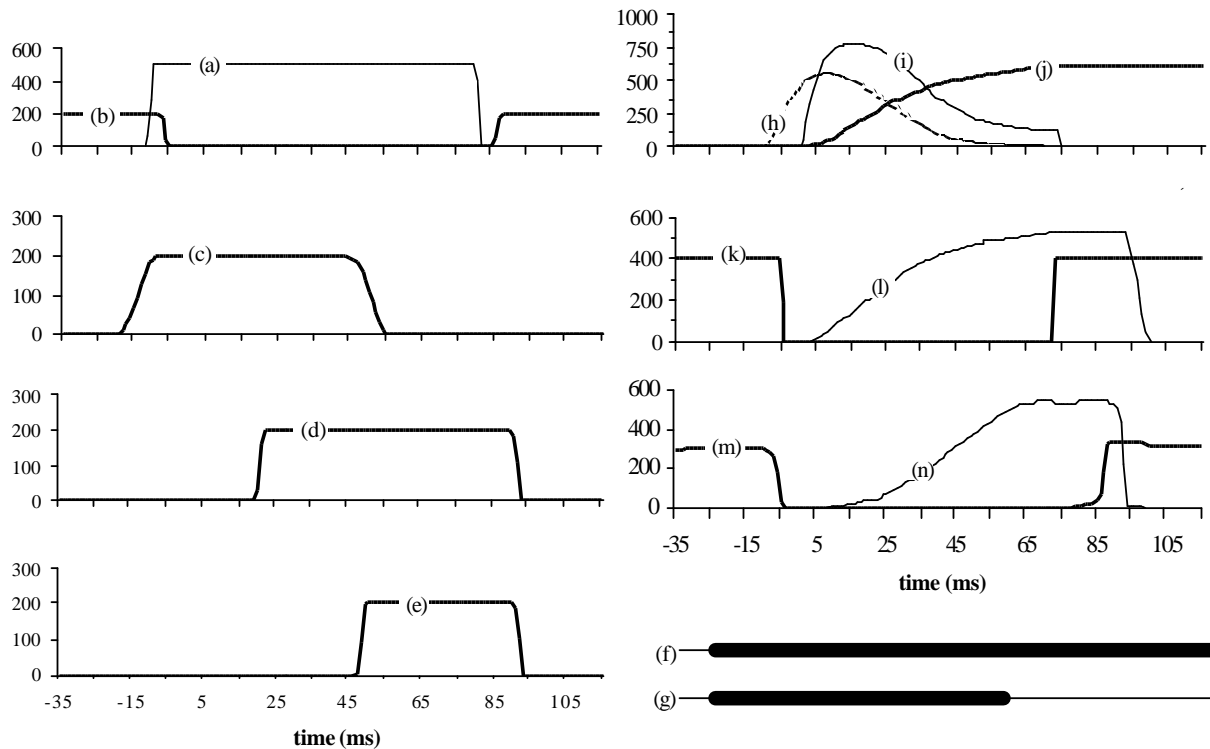
Fig. 4. Activity profile of some model's processing units in a simple saccade context. Left column. Activity profile of single SC cells for a simple 22 deg express saccade. Vertical axes: Model estimate of the firing rate (spikes/s). (a) A Saccade-Related Burst Neurons (SRBN) with maximal response across the SRBN lamina. (b) A rostral Movement- Coding Related Neuron (rM-CRN). (c)-(d)-(e) Three caudal Movement-Coding Related Neurons (cMCRNs) whose positions in the motor map corresponds to saccades of 22deg, 10deg and 5deg respectively (in nominal conditions). For a comparison with existing experimental results, see [46, Fig.1,p.2337]. (f) Visual stimulus. (g) Input to SC intermediate layer. **Right column.** Activity profile of brainstem inputs and saccade-related cells for a simple 22deg express saccade. (h) Long-lead burst neurons (LLBNs). For a comparison, see [63, Fig.11,p.344]. (i) Excitatory burst neurons (EBNs). (j) Tonic neurons (TNs) (arbitrary unit). (k) Omnipause neurons (OPNs). (l) Resetable integrator (RI). (m) OPN input from SC-rMCRNs. (n) OPN input from SC-cMCRNs.

Other working hypotheses are also embedded in the model. A dynamic, motor-error feedback loop, local to the brainstem is hypothesised, as in other modeling reference works [30, 57, 61]. This implies the integration of the motor-command signal issued from EBNs by a hypothetical Resetable Integrator (RI) and the estimation of a motor error by means of Comparator Neurons (CNs) receiving as inputs the desired displacement (from SC-SRBNs) and the estimated displacement (from RI); see Fig.3 EBN→RI→CN→OPN. The output from RI projects to both CNs and LLBNs, as do Inhibitory Burst Neurons in [62], causing a gradual decrease of LLBN activity as the movement proceeds. OPNs are known to project extensively onto EBNs [6, 68], and to act as a tonic inhibitory gate for the saccade burst generator [28]; hence the inhibitory projection from OPNs to EBNs in the model. Finally, the last two modeling hypotheses consist of an inhibitory projection from OPNs to RI (responsible of a gradual decrease of activity of the latter neurons at or near saccade termination), and an axonal- blockading signal s2 operating at the level of this projection. The latter hypothesis aims at preventing any accidental reset of RI before full comple-

tion of the saccade, as it is the case in experiments where OPNs or SC-RMCRNs are subject of direct electrical stimulation [4, 31, 33, 47].

Production of Two-Dimensional Saccades. The saccadic system as described in Fig.3 is capable of generating saccades in the azimuthal plane, and in one direction only. Its extension to the general, binocular, two-dimensional case is depicted Fig.6. It is composed of four main blocks, each of which is strictly identical to the saccadic system described previously and illustrated in Fig.3. The place code originating from the SC-SRBN layer is decomposed into vertical and horizontal components (see (9) in sec.7.3). As far as horizontal movements are concerned, four muscular groups are involved. The lateral recti (LR) move the eye in the temporal direction (the right eye to the right and the left eye to the left) and the medial recti induce movements in the nasal direction. Targets falling in a given visual hemifield (e.g. right) are processed by the contralateral SC (left), which activates the corresponding brainstem saccade generator (left), which in turn sends excitatory signals to both ipsilateral MR (so that the left eye turns to the right) and contralateral LR (so that the right eye also turns to the right).
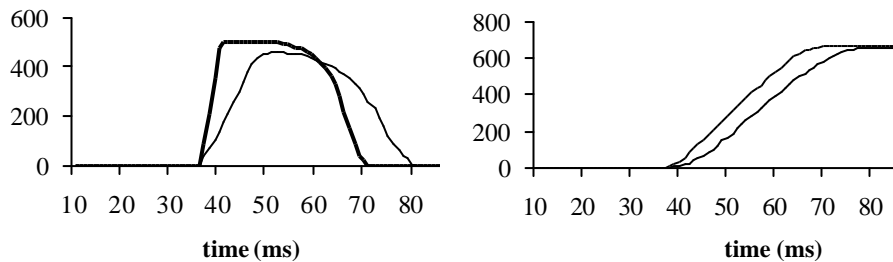
Fig. 5. Example of modulation of saccade dynamics for a 22 deg visual target. Left chart: Activity of Excitatory Burst Neurons (EBNs). **Right chart:** Activity of Tonic Neurons (TNs) (arbitrary unit). For a comparison with existing experimental results, see [67, e.g. Fig.3, p.3364]).

3   Implementation

3.1   Hardware

The experimental robotic platform used for the present study is a Nomadic Technologies XR4000, known in our lab under the casual name of Zakariah, and more often referred to using its nickname Zak (see Fig.7left). It is composed of the original XR4000 platform, on top of which a metallic structure of a custom design has been installed, which serves multiple purposes. In this particular case, two cameras (SUPER CIRCUITS PC-33C) are mounted on two pan and tilt units (Directed Perception, PTU-46- 17.5), which themselves are fixed on top of Zak's customized upper part. On the computing power side, Zak is equipped with two dual Pentium backplanes, the upper one being dedicated to user- customized developments. The latter computer is equipped of a video capture card for the acquisition and conversion of the video signals originating from both cameras.
 The two stepping-motors of each pan and tilt unit (one motor per degree of freedom) are driven by two controllers receiving digital commands from the upper computer through the serial line and transforming them into appropriate stepping commands.

3.2   Software Implementation

Zak's upper computer has been installed with Windows NT as an alternative operating system (in addition to the original Linux OS). The model and its interface with the video capture card and the pan and tilt units have been entirely developed as a multithreaded Windows NT application using Microsoft Visual-C++.
The major problem encountered related to the mode of control of the pan and tilt units. On the one hand, one of the main aspects of this study is to provide camera movements that resemble human eye velocity profiles, and on the other hand our pan and tilt units are equipped with stepping motors (as opposed to analog motors). The set of user commands and parameters accepted by the pan and tilt controllers include absolute and relative position shifts, speed, acceleration, trapezoidal velocity profile and on-the-fly changes of position and speed (but not acceleration).
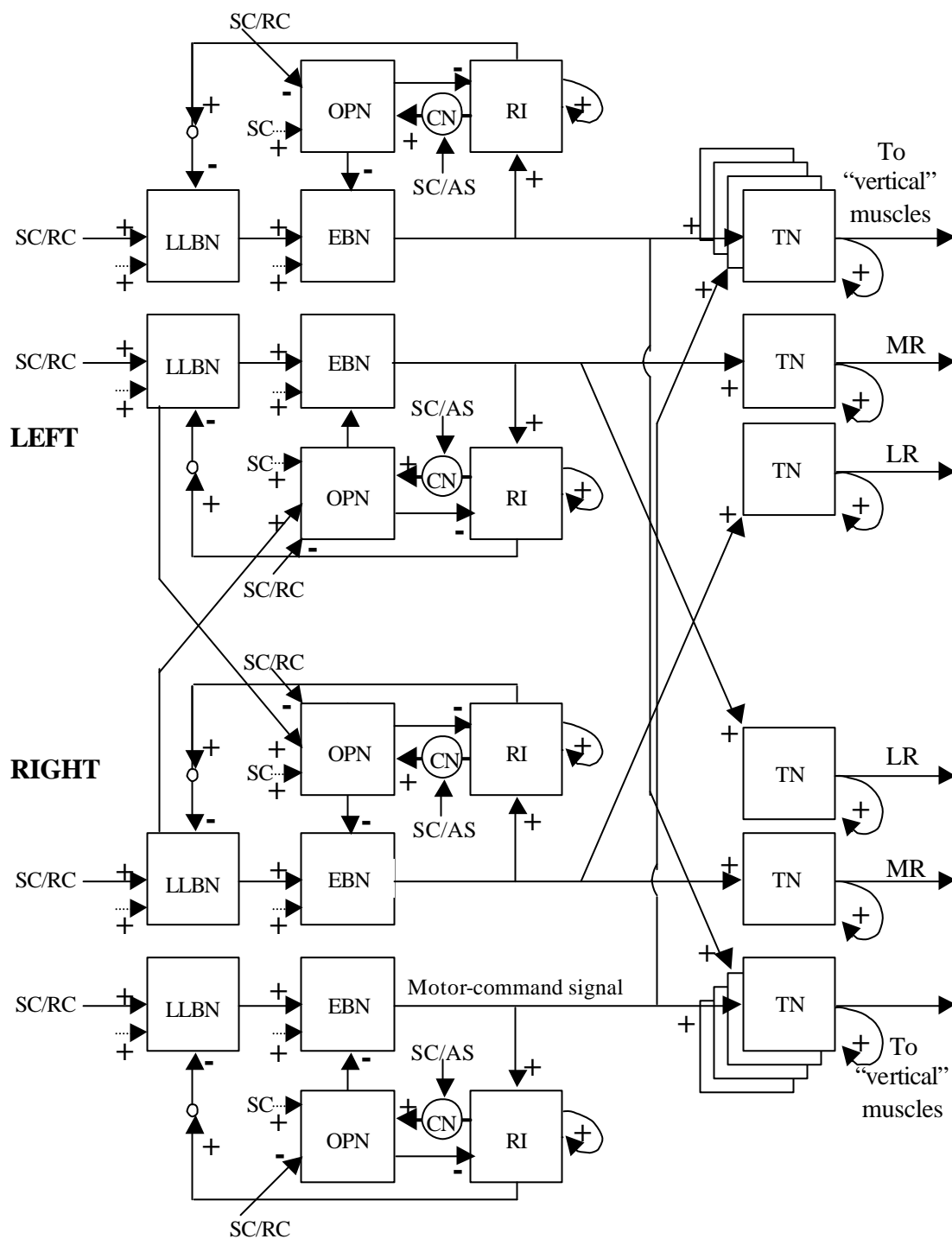
Fig. 6. Brainstem circuitry for movements in all directions (both eyes). LLBN: Long-Lead Burst Neurons. EBN: Excitatory Burst Neurons. OPN: Omnipause Neurons. RI : Resetable Integrator. CN: Comparator Neurons. TN : Tonic Neurons. LR : Lateral Rectus muscle. MR : Medial Rectus muscle. SC: Superior Colliculus (In front of arrows to OPNs, SC stands for SC-MCRNs). SC/AS: Amplitude signal calculated from the place (population) code at the level SC-CRBNs. SC/RC: Superior Colliculus Rate Code.
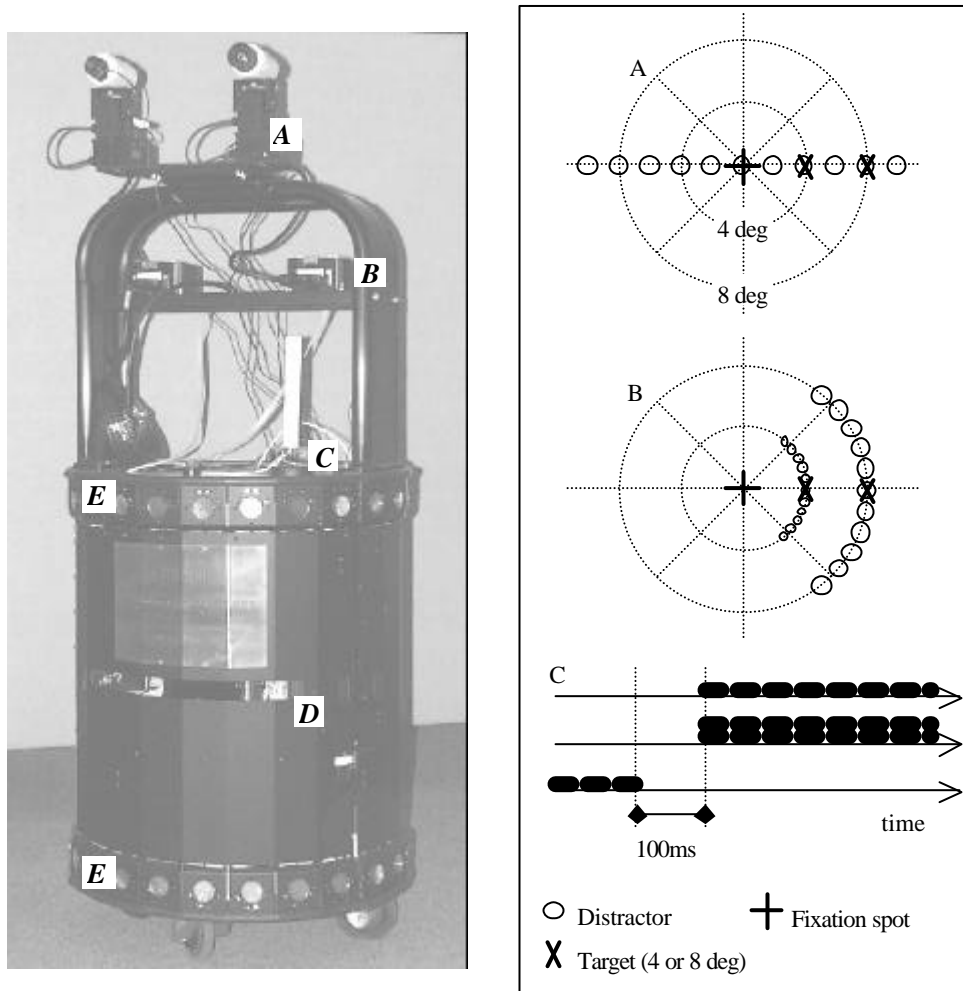
Fig. 7. Left picture: Zakariah. The cylindrical lower part is the original XR4000 mobile robot (by Nomadic Technologies), including two belts of ultrasonic, infrared and pressure sensors (E), a laser range finder (D) and a wireless ethernet antenna (C). The upper part metallic structure is of a custom design. Two pan and tilt units (A) (by Directed Perception), connected to two pan and tilt controllers (B) (same origin), provide motion to two cameras (SUPER CIRCUITS PC-33C). **Right picture: Experimental setup (synthetic and real-world signals).** Panels A and B (corresponding to experiments A and B respectively) show the relative positions between the target and the distractor (there is only one target and one distractor per scenario). As depicted on panel C, the target and the distractor are simultaneously switched on, about 100 ms after a fixation stimulus (located at the centre of the visual field) has been turned off.

In other words, facilities needed by this study for illustration purposes, such as on-the-fly acceleration change or preset of user-customized velocity profiles, are not available. This problem has been overcome the following way. All equations of the model remain the same, including EBNs. But a user-defined step is used to quantize the velocity command (EBN output). On-the-fly speed change commands are sent to the pan and tilt controllers each time the analog EBN output signal reaches a different quantization level.

Several purpose-dependent implementations of the model have been integrated in a single program (namely a multithreaded Windows NT application): a stand-alone version of the model for tests based on synthetic data (or video signals read from a file), a run-time version interfaced with the video camera and the wheel motors of a Khepera micro-robot (controlled from a remote computer), and an inboard, run-time version for the control of Zak's cameras; the way the model equations are coded being strictly identical from one version to the other. In other words, experimental results presented in the next section are based on the same computer code, regardless of the experimental context itself (synthetic data vs. real world seen through Zak's eyes). The architecture of the Zak-dedicated code consists of two threads (aside from the application main thread). Thread A is an asynchronous loop including the calculation of an estimate of the first (temporal) derivative of the gray-level component of the video signal, the approximate elapsed processing time of the loop being user-defined. Thread B is a loop including the update of all other equations (see (1) and (2) in sec.7), including the motor commands and the retinal GCs, which take as input the quantity computed in thread A. Thread B operates the quantization of the velocity signal (EBN output) and sends the corresponding motor command to the pan and tilt controllers through the serial line.

4   Experiments

4.1   Effect of a Remote Distractor onto Saccade Latency and Amplitude

The experimental setup that was used to study the effect of remote distractors in saccade programming is depicted Fig.7right. The basis paradigm consists in simultaneously switching a target and a distractor on, about 100 ms after a fixation stimulus (located at the centre of the visual field) has been turned off, as depicted Fig.7rightC. In experiment A, targets were located on the azimuthal axis, either at 4deg or 8deg from the centre and distractor positions were varied along the same axis, from 10deg to +10deg with increments of two degrees (see Fig.7rightA). In experiment B, targets had the same locations as in experiment A, and were presented simultaneously with targets of constant eccentricities (either 4deg or 8deg) and varied orientations (from -50deg to +50deg, with 10 degrees increments) (see Fig.7rightB). The two following situations were considered: 4deg target eccentricity and 8deg distractor eccentricity, noted T4D8, and the symmetric one, noted T8D4.

In experiments making use of synthetic visual signals, the visual scene consisted of a uniform, 'black' background where only three cells of the photoreceptor array were varying over time: the centered fixation spot, the flashing target and the flashing distractor (Fig.7rightC). The maximum intensity of the synthetic signal corresponding to the target was greater than for the distractor and the fixation spot. Saccadic reaction times were measured indirectly as the number of numeric integration steps (i.e. number of loop iterations) between target onset and onset of EBN activity (velocity signal). Saccade amplitudes were estimated by performing an integration of the analog velocity command signal. The real-world experimental setup followed exactly the same paradigm. Likewise, the maximum intensity of the light bulb corresponding to the target was greater than the other two. For each target/distractor pair, a video film was recorded in a file, using a temporal sampling rate set to the same duration as the usual periodicity of the video capture in thread A (namely 20ms). The model reaction time was estimated indirectly using the off-line version of the model, by playing the film step by step and by counting the number of numeric integration steps between the target onset and onset of EBN activity. Distractor effects on saccade amplitude (and orientation) were measured using the double- threaded run-time version of the model. Saccade amplitudes were estimated by performing a temporal integration of the discrete velocity command signals sent to the pan and tilt units.

4.2   Results

The data collected for experiment A are reported 8. The experimental conditions are sufficiently close to those of experiment 1a described in [74] for the results to be compared. For sake of clarity, corresponding data of [74, Fig.3A&B p.1112] have been redrawn here in 8A&D respectively.

The observed dependence of Saccade Reaction Time (SRT) on the eccentricity of contralateral distractors (Fig.8B&C) is a direct consequence of the crossed, inhibitory projection scheme between colliculi of both hemispheres (Fig.1B). For the purpose of this study, the corresponding synaptic weighting have been determined according to the position of the cell on the rostro-caudal axis. This synaptic strength increases (hyperbolically) with proximity to the rostral pole, hence the observed peak in saccade latency for distractors located exactly at the center of the visual

field. When both target and distractor share the same hemifield, measured SRTs compare with SRTs obtained for saccades induced by single targets of similar eccentricities. The global shift in SRT observed in experiments based on real-world scenarios (8C) can be explained in terms of the presence of a background noise, which results in an increase of the global activity at the level of SC-MCRNs, which in turn induces a reinforcement of their inhibitory action onto contralateral SC-SRBNs and onto ipsilateral SC-SRBNs (because of the inhibitory projection from rostral SC-MCRNs). In the present model, the effect of a remote distractor on saccade amplitude (8E&F) is not a consequence of any processing upstream of SC. Consistently with the experimental evidence presented in [14], the averaging of the target/distractor pair is performed in the neural network situated downstream of SC (see the *population decoding* functional unit Fig.3; see also (7) in sec.7.3). The averaging is asymmetrically weighted, with weight strength (hyperbolically) decreasing with increasing eccentricity (see (11) and (9) in sec.7.3).
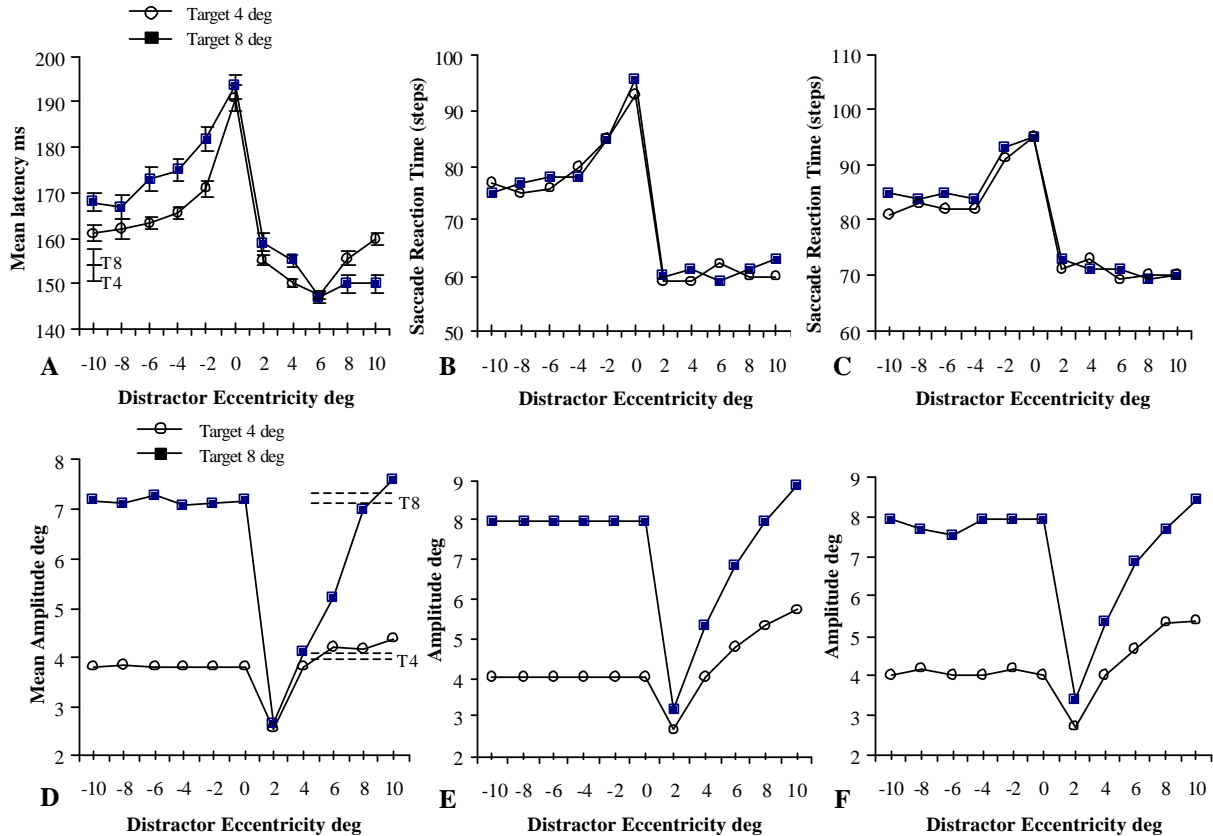
Fig. 8. Effects of remote distractors on saccade reaction time (left column) and amplitude (right column) for experiment A. A&D: Data redrawn from [74, Fig.3A&3B,p.1112]. B&E: Results based on synthetic data. C&F: Results based on real-world data.

Data collected according to the paradigm B (see Fig.7rB) are shown Fig.9, where Fig.9A shows data redrawn from [74, Fig.7B,p.1114]. These results demonstrate the effect of distractor orientation on saccade accuracy. In all cases, target and distractor belong to the same visual hemifield. This effect is noticeable when the target and distractor axes form an angle smaller than 20deg and reaches its maximum when the target, the distractor and the fixation spot are aligned (provided that the ratio between their eccentricities remains within a certain range). In these conditions, the eye lands at a location that is a weighted average between the target and the distractor locations (always closer to the less peripheral visual event). In the present model, this effect is also a direct consequence of the population decoding functional unit situated downstream of SC. The degradation in accuracy that can be observed between synthetic and real-world data (Fig.9B vs. 3C) can be explained by the size of the spread of activity caused by a simple visual event (either distractor or target) that is significantly larger in the case of real-world stimuli.
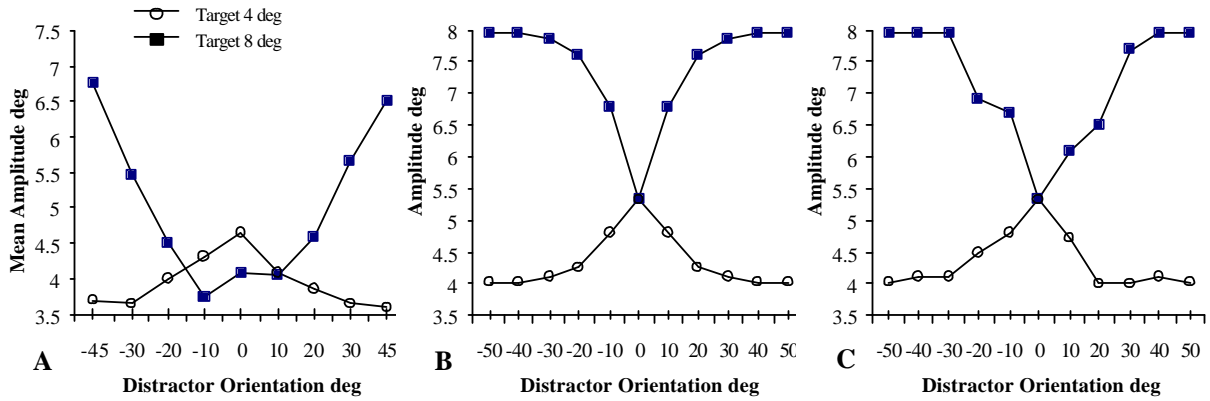
Fig. 9. Effects of relative position between target and distractor on amplitude (experiment B). A: Data redrawn from [74, Fig.7B,p.1114]. B: Plot of experiments based on synthetic data. C: Results based on real-world data.

4.3   Component Stretching

Under normal conditions trajectories of saccadic eye-movements are straight [48]. On the other hand, at the mechanical level, horizontal and vertical movements are provided by two separate groups of oculomotor muscles. Thus, in order to achieve straight oblique saccades, the brainstem saccade generator has to stretch the duration of the movement whose component is the smallest. In the present model, vertical and horizontal saccade generators are driven by the rate code signals originating from SC (Fig.3&6). These signals derive from the global activity of the SC-SRBN population and are weighted by the cosine (horizontal component) or the sine (vertical component) of the angle between the target and the azimuth axes (see (11) in 7.3). Hence, for a given component, saccade parameters such as duration and peak velocity vary according to the target angle. Figure 10 shows an example of
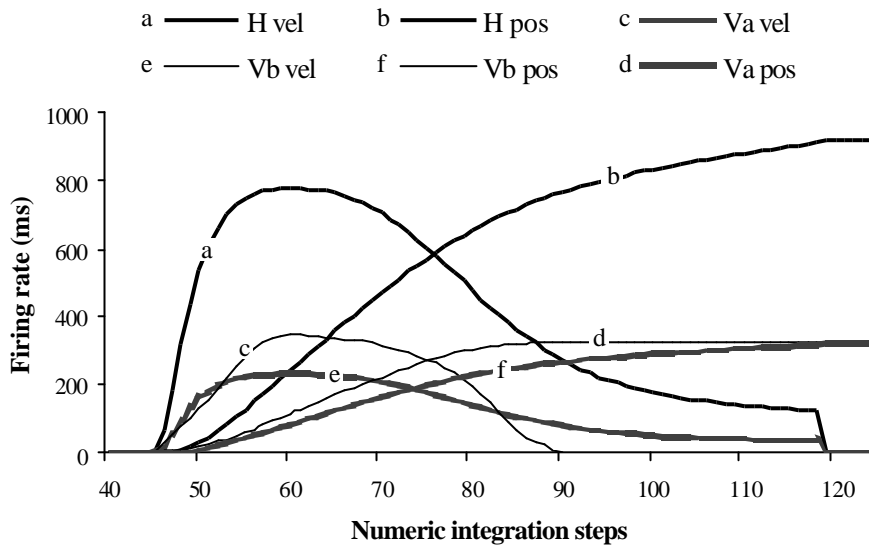
Fig. 10. Component stretching. While programming an oblique saccade (in this case amplitude=25deg and orientation=30deg), the model stretches the component of lowest amplitude. Curve (e) shows the vertical velocity signal (EBN activity) for this oblique movement. Curve (c) shows the vertical velocity signal obtained for a purely vertical movement whose amplitude equals the vertical component of the oblique movement. Curve (a) shows the horizontal velocity signal for this oblique movement. Curves (f), (d) and (b) plot the eye position profiles (TN activity) corresponding to (e), (c) and (a) respectively (arbitrary unit).

two saccades produced by the model, one purely vertical and one oblique, both of them involving the same amount of displacement at the level of the vertical component.

In the case of the oblique movement, the duration of the vertical movement has been stretched (and the peak velocity decreased) in order to match the horizontal movement's onset and end.

5 Discussion

5.1 Human Oculomotor Plant Properties vs. Actuation Mechanisms of the Video Input Device of a Humanoid

The human eye-plant is commonly simulated as a second-order system (see (12) in appendix), as originally proposed in [56]. However, a recent series of thorough studies has showed that the identification of the transfer function that maps the neural signals responsible for optic saccades into the eye-position itself (as the output, time-varying signal) is an extremely complex problem [10]. In other words, the detailed description of the oculomotor plant properties and its driving neural signal is a task which is still under progress.

In the present study, we have set the focus on the identification and implementation of computational principles that result in providing a humanoid robot with behaviours which, seen by a human observer, appear as human-like as possible. However, the issue of the actuation mechanisms of the video camera has been deliberately left apart, as it constitutes an area of research in itself. From an engineering perspective, the human eye is a system capable of smooth motions over a broad range of velocities; with a peak speed of about 800 deg/s that can be reached in a few tens of milliseconds. But the technical specifications of the actuation mechanism of a humanoid "eye" do probably not need to replicate the peculiarities of its human counterpart in order to achieve human-like "eye"-movements and gaze-related behaviours. For example, some movements such as express saccades are so quick that the smoothness of the movement can not be perceived by a human observer. However, some information can still be extracted by a human observer from an express saccade, such as the latency and the landing location; both of which having been addressed in the present study.

A second category of eye-movement is smooth-pursuit, where the eye operates at a speed-range much lower than optic saccades. In this case, the smoothness of the motion is a crucial prerequisite for any artificial actuation mechanism that aims to produce human-like motions.

Consequently, as far humanoid design is concerned, any technology is suitable (e.g. analogous, step-wise, etc.) as long as it enables the production of smooth movements; at least within the range of velocities where their natural counterpart are perceived as smooth by a human observer. In other words, more psychophysical data is needed in order to quantify how the eye-movements of a first human being are perceived by another human observer.

5.2 Scalability

In this study, several properties of the saccadic system in humans (or primates in general) have been investigated, including the effect of the increase of complexity in a visual scene (number of potential targets) on reaction time and eye-movement programming. All of them directly contribute to the development of humanoid robots for they provide such systems with motions (in this case horizontal and vertical eye-movements) and behaviors (in this case, gaze orientation) that closely resemble their human counterparts.

In other words the latter properties demonstrate the similarity of the model to the biological case from the point of view of an external observer. In addition, at the structural level this time, the same model embeds the most recent evidence and hypotheses of circuitry and physiology concerning both SC and brainstem saccade generator. Most of its functional units replicate neural activity profiles observed in primates. Moreover, it has been demonstrated to account for several other structural properties such as on-the-fly saccade interruption/resumption through direct electrical stimulations of SC rostral MCRNs and RIP OPNs, staircase-like eye-movements caused by direct, sustained electrical stimulation of SC- SRBNs, and modulation of saccade dynamics (peak velocity and duration).

As a result, the present model should be seen as a modular integration platform that can be easily modified and extended in order to host additional functional units. For example, the general, binocular, two-dimensional saccadic system (that allows the production of straight oblique saccades) is made of four separate functional blocks of identical structure. Another example regards saccade reaction time, where the simple addition of a (biologically-plausible) crossed inhibitory projection between colliculi of both hemispheres allows to account for several psychophysical effects (e.g. latency increase according to distractor position).

In terms of forthcoming extensions, the structure of the present model is already organized in order to permit the addition of several functional units. More refined strategies of saliency detection and gaze-holding can be integrated by further modeling of the indirect pathway from GCs to SCd through the parietal and frontal lobes (without loss of phenomena already accounted for by the model). The contribution of the spatial information originating from the auditory channel can be integrated to the model by simple structural modifications at the SCd level (namely, at

the level of the equations of SC-SRBNs and SC-MCRNs). Adaptation and learning capabilities can be added by integrating a cerebellum model acting at the level of SCd, LLBNs and EBNs (see external inputs EMIb, EMId and EMIe, Fig.3). The latter addition would be particularly important for the extension of the present system towards the combined control of head and eye- movements.

5.3   Software vs. Hardware

Almost all the processing performed in the experiments described in this paper are done in software on desktop type computers. This may appear non-neuromorphic to some, but we believe exploring and testing hypotheses and architectures, in particular complex ones, ought to be done in software. In fact with the rapid progress in digital signal processors (e.g. see the Lucent/Motorola StarCore DSP or the Texas Instrument TMS320C62X series) and microprocessor technologies, it is hard to argue for special integrated circuits except when they will provide superior performance not only at the time of their design, but also in the years that follow in their utilization.
An important aspect of neuromorphic research is the ability to extend the operational life (whether for explorative research or for actual operations) beyond the initial laboratory testing. Using standard programmable components like DSPs or microprocessors allow researchers to ride on the back of continuous improvements the manufacturers provide and that Moore law predicts.
Another important aspect of software programmability is the ease with which algorithms, in particular those related to learning can be implemented without committing to very expensive and time enduring design processes typically required for hardware based solutions.
The arguments above are not discounting the possibility of using specialized and opportunistic microelectronic solutions to implement biological functions. We are simply arguing that committing to analog or digital microelectronic implementation could be delayed until more complex architectural issues no longer represent the obstacles, in then one would consider the real advantages of developing specialized integrated circuits.

5.4   Designing Humanoids with Gaze-Shifting Properties similar to Humans: Issues and Challenges

As pointed out in the beginning of this section, one of the most important priorities in the design of humanoids is the degree of naturalness in the robot behaviour. In terms of gaze-shift tasks, this naturalness extends beyond the simple scope of kinematic and dynamic properties. One should bear in mind that the control of the system of eye-movement in humans is shared between voluntary and involuntary responses. The configuration of this system is such that a voluntary task, such as tracking a moving object (with the clear instruction not to look at anything else but the object) can be interrupted momentarily by any sudden, salient visual stimulus such as a light flashing (or by auditory stimuli): A different, reflexive, involuntary control system takes over and redirects the line of sight for a moment, or permanently, according to the properties of the stimulus. The naturalness of gaze-shift tasks of a humanoid would probably judged too poor if the robot is not able of mixing these involuntary and voluntary responses. Another example of a property of the human gaze-shifting system is the randomness in the saccadic-reaction time (on a trial-by-trial basis). The latter quantity can vary dramatically for repeated trials of a given experiment under non-varying laboratory conditions. One of the most popular theory explaining this phenomenon is based on an evolutionary argument, for this randomness can increase the difficulty for a predator to predict and learn prey's visuomotor responses. Whether or not a humanoid is endowed with such a property (randomness in saccadic reaction-time) might also influence how natural its gaze-shifting responses appear to a human observer. More generally, the new field of humanoid design would certainly benefit from psychophysical studies identifying what properties of the gaze-shifting system are important in regard of the naturalness of the behaviour.
A second important question concerns the relationship existing between the physiology and movements of the human eye; for example, the fact that the retina performs a non-homogeneous spatial sampling, with highest resolution at the center (the fovea), or the fact that the neural visual signal carried by the optic nerve fades away in absence of motion. While the movement of the eye is something perceivable by an external human observer, the way the visual signal is acquired and processed is not. Therefore, the legitimate question arises to what the benefit is of replicating the physical properties of the human eye, when considered as a light sampling device. The latter question can actually be extended to all brain areas responsible in the processing of visual stimuli. And, as in all "airplanes-don't-flap-wings" problematics, the answer always depend on the level of achievement of the state-of-the-art. In the particular case of humanoid design, it seems that a lot of problems remain unsolved. Therefore, any path is worthwhile going down and the computational brain modelling approach is one of them.

5.5 Contribution of Neuromorphic Engineering to the Design of Humanoids

One can ask the question of what the differences between neuromorphic engineering and humanoid design research are. If one assumes that neuromorphic engineering is not only concerned with analog VLSI based solutions to implement biological functions, but is about the artificial implementation of biological functions using models that closely resemble their biological counterparts, one would argue that neuromorphic engineering is a processor (possibly the natural process) in progressing towards humanoid systems. Over the last decades, neuromorphic engineering focused mainly on the microelectronic implementation of peripheral subsystems (retina, cochlea, simple saccade systems). However as progress is made towards the modeling and implementation of mid-brain, sub-cortical and cortical functions, as well as the mechanical actuators, neuromorphic engineering will become concerned with the hardware and software backbones of humanoid systems.

6 Conclusion

We have presented a system that is capable of replicating several properties of gaze-shifting in human, thus capable of reproducing natural movements (eye-movements) and natural behaviors (effect of visual scene complexity on reaction time and target selection). This system has been successfully implemented and demonstrated on a Nomadic Technology XR4000 robotic platform. It is based on a computational model of the main neural pathway for saccadic eye-movements in primate. The latter embeds the most recent evidence and hypotheses of circuitry and physiology concerning both the superior colliculus and the brainstem saccade generator, and has been shown to account for numerous electrophysiological and behavioral observations. More generally, because of its modular, biologically-inspired structure, the present system represents a first step towards a more complete picture of orientation behaviors in human, such as the coordination of eye-, head- and body-movements in response to behaviorally-significant stimuli originating from somatosensory, auditory and visual sensory channels (the integration of the auditory component being currently under progress). In this regard, further advances in the understanding of robotic-relevant computational principles of brain centers such as the cerebellum, the basal ganglia and the frontal lobe are of particular importance.

7 Appendix

7.1 Firing Rate Model

Unless otherwise stated, neuron responses were estimated using a firing rate model:

$$\frac{dX(t)}{dt} = -\frac{X(t)}{\tau} + \frac{I(t)}{\tau} \tag{1}$$

$$Y(t) = F_A(X(t)) = \begin{cases} 0 & \text{if } x < 0 \\ A\left(\frac{1}{2} + \frac{1}{2}\sin\left(\frac{x}{A}\pi - \frac{\pi}{2}\right)\right) & \text{if } 0 \le x \le A \\ A & \text{otherwise} \end{cases} \tag{2}$$

where $X(t)$ represents the neuron's state (function of the membrane potential) at time t, $I(t)$ the weighted sum of its inputs and $Y(t)$ an estimate of its instantaneous firing rate. The symbol τ stands for the neuron's time constant. A designates the neuron's maximum firing rate. The function F is sigmoidal positive. In the present study, the numeric integration of model's equations consisted of the first order approximation of (1).

7.2 Retinal Ganglion Cells

The gray-level component of the video signal is stored in a two-dimensional $(N \times P)$ array. In a standard XY Cartesian reference system, the centered coordinates of a given (k, l) cell of the video signal array are $(l - C_x, k - C_y)$, with $C_x = P/2$ and $C_y = N/2$ (see figure 3). A second array of identical organization is used to store the estimates of the instantaneous (temporal) derivative for each cell of the video signal array (refered to as the photoreceptor array in Fig.2). The activity of the retinal ganglion layer is stored in a two-dimensional $(Q \times R)$ array, lying in a log-polar coordinate system. Each (q, r) cell of this array is associated to a weight matrix that defines a receptive field in the photoreceptor array, the coordinates of the center of this receptive field being $(\rho\cos\theta, \rho\sin\theta)$:

$$\begin{aligned} \rho &= K \cdot \left(\exp\left(\frac{r-0.5}{B} - 1\right) - 1\right) \quad 1 \le r \le R \\ \theta_{\deg} &= 90 - \frac{180 \cdot (q - 0.5)}{Q} \qquad 1 \le q \le Q \end{aligned} \tag{3}$$

GC activities are calculated as follows (unlike the general principle of activity update presented above):

$$GC_{q,r}(t_n) = \begin{cases} F_{t_n}(GC_{q,r}(t_{n-1})) + u_{q,r}(t_n) & \text{if } u_{q,r}(t_n) > 0 \\ F_{t_n}(GC_{q,r}(t_{n-1})) & \text{otherwise} \end{cases} \tag{4}$$

with

$$u_{q,r}(t_n) = \frac{d}{dt}\sum_{k=1}^{N}\sum_{l=1}^{P} W_{k,l}^{q,r} ph_{k,l}(t_n) = \sum_{k=1}^{N}\sum_{l=1}^{P} W_{k,l}^{q,r}\frac{d}{dt}(ph_{k,l}(t_n))$$

$$F_T(GC_{q,r}(t_{n-1})) = GC_{q,r}(t_{n-1}) \cdot \exp(-\alpha(T - t_{n-1}))$$

where

- t_n is the time stamp corresponding to the capture of video frame number n,
- $GC_{q,r}(t_n)$ is the value of the output activity of the (q,r) ganglion cell, whose receptive field centre is located at radius ρ and orientation θ from the center of the photoreceptor layer (at time t_n),
- $ph(t_n)$ is the gray-level component of the video frame captured at time t_n,
- $W^{q,r}$ is the GC receptive field weight matrix associated to the (q,r) ganglion cell, whose values are the difference of two gaussian distributions of different radii and amplitudes:

$$W_{k,l}^{q,r} = k_c^{gc} \cdot \exp(\frac{d_{k,l,\rho,\theta}^2}{(\sigma_c^{gc})^2}) - k_r^{gc} \cdot \exp(\frac{d_{k,l,\rho,\theta}^2}{(\sigma_r^{gc})^2}) \tag{5}$$

$$d_{k,l,\rho,\theta}^2 = ((l - C_x) - \rho\cos\theta)^2 + ((k - C_y) - \rho\sin\theta)^2 \tag{6}$$

7.3 Decoding of the SC-SRBN Place & Rate Population codes

In the present model, the neural network responsible for the decoding of the SC-SRBN place and rate codes consists of retinotopic array of $Q \times R$ cells. Each individual cell receives excitatory projections from SC-SRBNs via its receptive field:

$$I_{q,r}^d(t) = k_1^d(W_{q,r} * Y^{\text{SC-SRBN}}(t)) + k_2^d I_{\text{lateral}}(t) - k_3\text{Bias}^d - k_4^u I_{\text{cancel}}(t) \tag{7}$$

with

$$W_{q,r} * Y^{\text{SC-SRBN}}(t) = \frac{1}{K_1^d}\sum_{i=1}^{Q}\sum_{j=1}^{R}\exp(\frac{(q-i)^2 + (r-j)^2}{(\sigma_1^d)^2})Y_{i,j}^{\text{SC-SRBN}}(t)$$

$$I_{\text{lateral}}(t) = \frac{1}{K_2^d}\sum_{i=1}^{Q}\sum_{j=1}^{R}\exp(\frac{(q-i)^2 + (r-j)^2}{(\sigma_2^d)^2})I_{i,j}^d(t)$$

The shape and size of the receptive fields directly influences the parameters of the averaging effect. The global inhibitory bias contributes to the overall winner-take-all dynamics by preventing the formation of remote, competitive poles of activity (and henceforth ascertains the presence of only one winning cluster of activity). The cancellation term $I_{\text{cancel}}(t)$ is the same signal which causes SC-SRBNs to stop firing at the end of the saccade cycle. This signal originates from rostral SC-MCRNs (*fixation* cells).

Let's denote (C_q, C_r), the coordinates of the barycentre of activity (of the winning cluster) and $Y^d(t)$, the global activity (the normalized sum of activity across the whole array). The displacement signals provided to both horizontal and vertical saccade generators ($DS_h(t)$ and $DS_v(t)$ respectively) are determined as the weighted projections on respective axes. Weights decrease hyperbolically with eccentricity (recall that the SCd structure is such that orientations are organized along an axis and eccentricities along the other).

$$DS_h(t) = \frac{1}{C_r} \cdot \cos C_q \tag{8}$$

$$DS_v(t) = \frac{1}{C_r} \cdot \sin C_q \tag{9}$$

Horizontal and vertical rate codes ($RC_h(t)$ and $RC_v(t)$ respectively) are determined as follows:

$$RC_h(t) = Y^d(t) \cdot \frac{1}{C_r} \cdot \cos C_q \tag{10}$$

$$RC_v(t) = Y^d(t) \cdot \frac{1}{C_r} \cdot \sin C_q \tag{11}$$

In practice, in order to produce straight oblique saccades in the most general range of situations, the balance between horizontal and vertical rate codes has to be fine-tuned by means of adaptable gains $G_h(C_q)$ and $G_v(C_q)$ (that are presumably under the control of the cerebellum). However, in the present study, straight oblique saccades of amplitudes ranging from 0 to 12 degrees could be directly obtained from 11 (that is without any such fine-tuning).

7.4   Other Components and Parameters of the Model

Equations, coefficient values and other details on the model implementation can be found and downloaded from
`http://www.sedal.usyd.edu.au/~sc/index.html`

7.5   The Oculomotor Plant

The primate eye plant is commonly modeled as a second-order system whose transfer function is (in the Laplace domain):

$$E(s) = \frac{1}{\tau_2 s^2 + \tau_1 s + 1} \tag{12}$$

with $E(s)$ the eye position, $\tau_1 = 0.15$ and $\tau_2 = 0.005$ as typical constant values.

Acknowledgements

References

[1] H. Aizawa and R. H. Wurtz. Reversible inactivation of monkey superior colliculus. i. curvature of saccadic trajectory. *J Neurophysiol*, 79:2082–2096, 1998.

[2] R. W. Anderson, E. L. Keller, N. J. Gandhi, and S. Das. Two-dimensional saccade-related population activity in superior colliculus in monkey. *J Neurophysiol*, 80:798–817, 1998.

[3] K. Arai, E. L. Keller, and J. A. Edelman. Two-dimensional neural network model of the primate saccadic system. *Neural Networks*, 7(1115-1135), 1994.

[4] W. Becker, W. M. King, M. Fuchs, R. Jrgens, G. Johanson, and H. H. Kornhuber. Accuracy of goal-directed saccades and mechanisms of error correction. In A. F. Fuchs and W. Becker, editors, *Progress in Oculomotor Research, Developments in Neuroscience*, pages 29–37. Elsevier, Amsterdam, 1981.

[5] B. Breznen and J. W. Gnadt. Analysis of the step response of the saccadic feedback: computational models. *Exp Brain Res*, 117(2):181–91, 1997.

[6] J. A. Buttner-Ennever and U. Buttner. A cell group associated with vertical eye movements in the rostral mesencephalic reticular formation of the monkey. *Brain Res*, 151(1):31–47, 1978.

[7] J. A. Buttner-Ennever and V. Henn. An autoradiographic study of the pathways from the pontine reticular formation involved in horizontal eye movements. *Brain Res*, 108(1):155–64, 1976.

[8] J. A. Buttner-Ennever and A. K. E. Horn. Neuroanatomy of the saccadic omnipause neurons in the nucleus raphe interpositus. In A. F. Fuchs, T. Brandt, U. Bttner, and D. S. Zee, editors, *Contemporary Ocular motor and Vestibular Research : A Tribute to David A. Robinson*, volume Buttner-Ennever95, pages 488–495. Thieme, Stuttgart, 1995.

[9] A. Cowey and P. Stoerig. The neurobiology of blindsight. *Trends Neurosci*, 14(4):140–5, 1991.

[10] K. E. Cullen and D. Guitton. Analysis of primate ibn spike trains using system identification techniques. i. relationship to eye movement dynamics during head-fixed saccades. *J Neurophysiol*, 78(6):3259–82, 1997.

[11] S. Das, N. J. Gandhi, and E. L. Keller. Open-loop simulations of the primate saccadic system using burst cell discharge from the superior colliculus. *Biol Cybern*, 73(6):509–18, 1995.

[12] P. Dean, J. E. W. Mayhew, and L. P. Learning and maintaining saccadic accuracy: A model of brainstem-cerebellar interactions. *J Cognit Neurosci*, 6(2):117–138, 1994.

[13] J. Droulez and A. Berthoz. Spatial and temporal transformation in visuomotor. In R. Eckmiller and C. von der Malsburg, editors, *Neural Computers*, pages 345–357. Springer-Verlag, Berlin, 1988.

[14] J. A. Edelman and E. L. Keller. Dependence on target configuration of express saccade-related activity in the primate superior colliculus. *J Neurophysiol*, 80(3):1407–26, 1998.

[15] S. Everling, M. Pare, M. C. Dorris, and D. P. Munoz. Comparison of the discharge characteristics of brain stem omnipause neurons and superior colliculus fixation neurons in monkey: implications for control of fixation and saccade behavior. *J Neurophysiol*, 79(2):511–28, 1998.

[16] B. Fischer and R. Boch. Saccadic eye-movements after extremely short reaction times in the monkey. *Brain Res.*, 57:191–195, 1983.

[17] B. Fischer and E. Rampsberger. Human express saccades: Extremely short reaction times of goal directed eye movements. *Exp. Brain Res.*, 57:191–195, 1984.

[18] G. Gancarz and S. Grossberg. A neural model of the saccade generator in the reticular formation. *Neural Networks*, 11(7-8):1159–1174, 1998.

[19] N. J. Gandhi and E. L. Keller. Spatial distribution and discharge characteristics of superior colliculus neurons antidromically activated from the omnipause region in monkey. *J Neurophysiol*, 78(4):2221–5, 1997.

[20] S. Grossberg and M. Kuperstein. *Neural Dynamics of Adaptive Sensory-Motor Control*. Pergamon Press, New-York, 1989.

[21] D. Guitton. Control of saccadic eye and gaze movements by the superior colliculus and basal ganglia. In R. Carpenter and C.-D. J.R., editors, *Eye-Movements. Vision and Visual Dysfunction.*, volume 8, pages 244–276. The Macmillan Press, London, 1991.

[22] D. Guitton, H. A. Buchtel, and R. M. Douglas. Frontal lobe lesions in man cause difficulties in suppressing reflexive glances and in generating goal-directed saccades. *Exp. Brain Res.*, 58:455–472, 1985.

[23] B. L. Guthrie, J. D. Porter, and D. L. Sparks. Corollary discharge provides accurate eye position information to the oculomotor system. *Science*, 221(4616):1193–5, 1983.

[24] V. Henn and B. Cohen. Coding of information about rapid eye movements in the pontine reticular formation of alert monkeys. *Brain Res*, 108(2):307–25, 1976.

[25] K. Hepp and V. Henn. Spatio-temporal recoding of rapid eye movement signals in the monkey paramedian pontine reticular formation (pprf). *Exp Brain Res*, 52(1):105–20, 1983.

[26] K. Hepp, V. Henn, T. Villis, and B. Cohen. Brainstem regions related to saccade generation. In R. Wurtz and M. Goldberg, editors, *The Neurobiology of Saccadic Eye-Movements*. Elsevier, Amsterdam, 1989.

[27] T. K. Horiuchi and C. Koch. Analog vlsi-based modeling of the primate oculomotor system. *Neural Comput*, 11(1):243–65, 1999.

[28] A. K. Horn, J. A. Buttner-Ennever, P. Wahle, and I. Reichenberger. Neurotransmitter profile of saccadic omnipause neurons in nucleus raphe interpositus. *J Neurosci*, 14(4):2032–46, 1994.

[29] P. J. Istvan, M. C. Dorris, and M. D. P. Functional identification of neurons in the monkey superior colliculus projecting to the paramedian pontine reticular formation. *Soc Neurosci Abstr*, 20:141, 1994.

[30] R. Jurgens, W. Becker, and H. H. Kornhuber. Natural and drug-induced variations of velocity and duration of human saccadic eye movements: evidence for a control of the neural pulse generator by local feedback. *Biol Cybern*, 39(2):87–96, 1981.

[31] E. Keller. Control of saccadic eye movements by midline brainstem neurons. In R. Baker and A. Berthoz, editors, *Control of gaze by brainstem neurons*, pages 327–336. Elsevier, New York, 1977.

[32] E. Keller. The brainstem. In J. R. Cronly-Dillon and R. H. S. Carpenter, editors, *Vision and Visual Dysfunction. Eye-Movements.*, volume 8, pages 200–223. The Macmillan Press Ltd, 1991.

[33] E. L. Keller and J. A. Edelman. Use of interrupted saccade paradigm to study spatial and temporal dynamics of saccadic burst cells in superior colliculus in monkey. *J Neurophysiol*, 72(6):2754–70, 1994.

[34] E. L. Keller and D. A. Robinson. Absence of a stretch reflex in extraocular muscles of the monkey. *J Neurophysiol*, 34(5):908–19, 1971.

[35] A. J. King, J. W. Schnupp, S. Carlile, A. L. Smith, and I. D. Thompson. The development of topographically-aligned maps of visual and auditory space in the superior colliculus. *Prog Brain Res*, 112:335–50, 1996.

[36] R. J. Krauzlis, M. A. Basso, and R. H. Wurtz. Shared motor error for multiple eye movements. *Science*, 276(5319):1693–5, 1997.

[37] P. Lefevre and H. L. Galliana. Dynamic feedback to the superior colliculus in a neural network model of the gaze control system. *Neural Networks*, 5:871–890, 1992.

[38] P. Lefevre, C. Quaia, and L. M. Optican. Distributed model of control of saccades by superior colliculus and cerebellum. *Neural Networks*, 11(7-8):1175–1190, 1998.

[39] E. S. Luschei and A. F. Fuchs. Activity of brain stem neurons during eye movements of alert monkeys. *J Neurophysiol*, 35(4):445–61, 1972.

[40] M. A. Meredith, J. W. Nemitz, and B. E. Stein. Determinants of multisensory integration in superior colliculus neurons. i. temporal factors. *3215-3229*, Journal of Neuroscience(7), 1987.

[41] M. A. Meredith and A. S. Ramoa. Intrinsic circuitry of the superior colliculus: pharmacophysiological identification of horizontally oriented inhibitory interneurons. *J Neurophysiol*, 79(3):1597–602, 1998.

[42] A. K. Moschovakis. Neural network simulations of the primate oculomotor system. i. the vertical saccadic burst generator. *Biol Cybern*, 70(3):291–302, 1994.

[43] A. K. Moschovakis and A. B. Karabelas. Observations on the somatodendritic morphology and axonal trajectory of intracellularly hrp-labeled efferent neurons located in the deeper layers of the superior colliculus of the cat. *J Comp Neurol*, 239(3):276–308, 1985.

[44] D. P. Munoz and P. J. Istvan. Lateral inhibitory interactions in the intermediate layers of the monkey superior colliculus. *J Neurophysiol*, 79(3):1193–209, 1998.

[45] D. P. Munoz and R. H. Wurtz. Saccade-related activity in monkey superior colliculus. i. characteristics of burst and buildup cells. *J Neurophysiol*, 73(6):2313–33, 1995.

[46] D. P. Munoz and R. H. Wurtz. Saccade-related activity in monkey superior colliculus. ii. spread of activity during saccades. *J Neurophysiol*, 73(6):2334–48, 1995.

[47] M. J. Nichols and D. L. Sparks. Component stretching during oblique stimulation-evoked saccades: the role of the superior colliculus. *J Neurophysiol*, 76(1):582–600, 1996.

[48] M. J. Nichols and D. L. Sparks. Independent feedback control of horizontal and vertical amplitude during oblique saccades evoked by electrical stimulation of the superior colliculus. *J Neurophysiol*, 76(6):4080–93, 1996.

[49] L. M. Optican. Adaptive control of saccadic and smooth pursuit eye-movement. In E. L. Keller and D. S. Zee, editors, *Adaptive Processes in Visual and Oculomotor Systems*, pages 313–320. Pergamon Press, Oxford, 1986.

[50] L. M. Optican. A field theory of saccade generation: temporal-to-spatial transform in the superior colliculus. *Vision Res*, 35(23-24):3313–20, 1995.

[51] M. Pare and D. Guitton. The fixation area of the cat superior colliculus: effects of electrical stimulation and direct connection with brainstem omnipause neurons. *Exp Brain Res*, 101(1):109–22, 1994.

[52] C. Quaia, P. Lefevre, and L. M. Optican. Model of the control of saccades by superior colliculus and cerebellum. *J Neurophysiol*, 82(2):999–1018, 1999.

[53] R. Rafal, J. Smith, J. Krantz, A. Cohen, and C. Brennan. Extrageniculate vision in hemianopic humans: saccade inhibition by signals in the blind field. *Science*, 250(4977):118–21, 1990.

[54] M. S. Raybourn and E. L. Keller. Colliculoreticular organization in primate oculomotor system. *J Neurophysiol*, 40(4):861–78, 1977.

[55] D. A. Robinson. Eye movements evoked by collicular stimulation in the alert monkey. *Vision Res*, 12(11):1795–808, 1972.

[56] D. A. Robinson. Models of the saccadic eye movement control system. *Kybernetic*, 14(2):71–83, 1973.

[57] D. A. Robinson. Oculomotor control signals. In G. Lennerstrand and P. Bach-y Rita, editors, *Basic mechanisms of ocular motility and their clinical implications*. Pergamon-Press, Oxford, 1975.

[58] M. Rucci, G. Tononi, and G. M. Edelman. Registration of neural maps through value-dependent learning: modeling the alignment of auditory and visual maps in the barn owl's optic tectum. *J Neurosci*, 17(1):334–52, 1997.

[59] P. H. Schiller, J. H. Sandell, and J. H. R. Maunsell. The effect of frontal eye fields and superior colliculus lesions on saccadic latencies in the rhesus monkey. *J. Neurophysiol.*, 57:1033–1049, 1987.

[60] P. H. Schiller and M. Stryker. Single-unit recording and stimulation in superior colliculus of the alert rhesus monkey. *J Neurophysiol*, 35(6):915–24, 1972.

[61] C. A. Scudder. A new local feedback model of the saccadic burst generator. *J Neurophysiol*, 59(5):1455–75, 1988.

[62] C. A. Scudder, A. F. Fuchs, and T. P. Langer. Characteristics and functional identification of saccadic inhibitory burst neurons in the alert monkey. *J Neurophysiol*, 59(5):1430–54, 1988.

[63] C. A. Scudder, A. K. Moschovakis, A. B. Karabelas, and S. M. Highstein. Anatomy and physiology of saccadic long-lead burst neurons recorded in the alert squirrel monkey. i. descending projections from the mesencephalon. *J Neurophysiol*, 76(1):332–52, 1996.

[64] A. C. Smit, A. J. Van Opstal, and J. A. Van Gisbergen. Component stretching in fast and slow oblique saccades in the human. *Exp Brain Res*, 81(2):325–34, 1990.

[65] D. L. Sparks. Translation of sensory signals into commands for control of saccadic eye-movements: role of the primate superior colliculus. *Physiol. Rev.*, 66:118–171, 1986.

[66] D. L. Sparks and R. Hartwich-Young. The deep layers of the superior colliculus. *Rev Oculomot Res*, 3:213–55, 1989.

[67] T. R. Stanford, E. G. Freedman, and D. L. Sparks. Site and parameters of microstimulation: evidence for independent effects on the properties of saccades evoked from the primate superior colliculus. *J Neurophysiol*, 76(5):3360–81, 1996.

[68] A. Strassman, C. Evinger, R. A. McCrea, R. G. Baker, and S. M. Highstein. Anatomy and physiology of intracellularly labelled omnipause neurons in the cat and squirrel monkey. *Exp Brain Res*, 67(2):436–40, 1987.

[69] A. Strassman, S. M. Highstein, and R. A. McCrea. Anatomy and physiology of saccadic burst neurons in the alert squirrel monkey. ii. inhibitory burst neurons. *J Comp Neurol*, 249(3):358–80, 1986.

[70] A. Strassman, S. M. Highstein, and R. A. McCrea. Anatomy and physiology of saccadic burst neurons in the alert squirrel monkey. i. excitatory burst neurons. *J Comp Neurol*, 249(3):337–57, 1986.

[71] A. J. Van Opstal and H. Kappen. A two-dimensional ensemble-coding model for spatial-temporal transformation of saccades in monkey superior colliculus. *Network*, 4:19–38, 1993.

[72] D. M. Waitzman, T. P. Ma, L. M. Optican, and R. H. Wurtz. Superior colliculus neurons mediate the dynamic characteristics of saccades. *J Neurophysiol*, 66(5):1716–37, 1991.

[73] W. J. Waleszczyk, C. Wang, W. Burke, and B. Dreher. Velocity response profiles of collicular neurons: parallel and convergent visual information channels. *Neuroscience*, 93(3):1063–76, 1999.

[74] R. Walker, H. Deubel, W. X. Schneider, and J. M. Findlay. Effect of remote distractors on saccade programming: evidence for an extended fixation zone. *J Neurophysiol*, 78(2):1108–19, 1997.